

Reaction of Cu^I with Dialkyl Peroxides: Cu^{II}-Alkoxides, Alkoxy Radicals, and Catalytic C–H Etherification

Raymond T. Gephart, III,[†] Claire L. McMullin,[‡] Nicholas G. Sapiezynski,[†] Eun Sil Jang,[†] Mae Joanne B. Aguila,[†] Thomas R. Cundari,^{*,‡} and Timothy H. Warren^{*,†}

[†]Department of Chemistry, Georgetown University, Box 571227-1227, Washington, D.C. 20057, United States

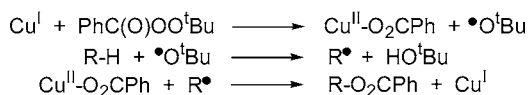
[‡]Department of Chemistry, Center for Advanced Scientific Computing and Modeling (CASCaM), University of North Texas, Denton, Texas 78203, United States

S Supporting Information

ABSTRACT: Kinetic analysis of the reaction of the copper(I) β -diketiminato [Cl₂NN]Cu ([Cu^I]) with ^tBuOO^tBu to give [Cu^{II}]-O^tBu (1) reveals first-order behavior in each component implicating the formation of free ^tBuO• radicals. Added pyridine mildly inhibits this reaction indicating competition between ^tBuOO^tBu and py for coordination at [Cu^I] prior to peroxide activation. Reaction of [Cu^I] with dicumyl peroxide leads to [Cu^{II}]-OCMe₂Ph (3) and acetophenone suggesting the intermediacy of the PhMe₂CO• radical. Computational methods provide insight into the activation of ^tBuOO^tBu at [Cu^I]. The novel peroxide adduct [Cu^I](^tBuOO^tBu) (4) and the square planar [Cu^{III}](O^tBu)₂ (5) were identified, each unstable toward loss of the ^tBuO• radical. Facile generation of the ^tBuO• radical is harnessed in the catalytic C–H etherification of cyclohexane with ^tBuOO^tBu at rt employing [Cu^I] (5 mol %) to give the ether Cy–O^tBu in 60% yield.

A number of metal-catalyzed C–H functionalization reactions employ organic peroxides as oxidants, often under mild conditions.¹ For instance, the Kharasch–Sosnovsky reaction (Scheme 1)² involves initial interaction between a

Scheme 1. Kharasch–Sosnovsky Reaction



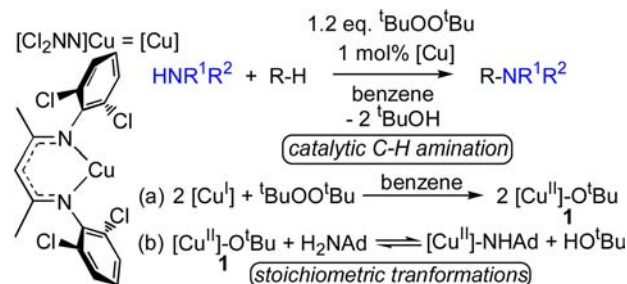
peroxyester such as PhC(O)OO^tBu with a Cu(I) source to give a Cu(II) benzoate Cu^{II}-O₂CPh with formation of ^tBuO•.^{3,4} This alkoxy radical engages in H-atom abstraction (HAA) reactions⁵ with R–H substrates (typically allylic) to produce a radical R• driven by the high O–H bond strength (BDE = 105 kcal/mol)⁶ of the corresponding alcohol ^tBuOH. The radical R• ultimately reduces the Cu^{II}-O₂CPh species to Cu^I with formation of the functionalized ester R-OC(O)Ph. High enantioselectivities in this C–H functionalization reaction⁴ may be achieved with bis(oxazolines)⁷ and other chiral ligands.⁸

Reaction between Cu(I) and peroxides can lead to diverse oxidized Cu species. Reaction of dibenzoyl peroxide with CuCl in pyridine gives both the divalent square planar CuCl-

(O₂CPh)₂py₂ and trivalent square pyramidal CuCl-(O₂CPh)₂py₂.⁹ Theoretical studies also supported possible oxidative addition of ^tBuOO^tBu to CuBr to give a CuBr(O^tBu)₂ intermediate¹⁰ in the C–H amidation of indoles.¹¹ A copper(III) alkoxy-carboxylate intermediate has been computationally considered in a radical-free variant of the Kharasch–Sosnovsky reaction.¹²

We recently reported a new protocol for catalytic C–H amination with simple alkyl¹³ and aromatic¹⁴ amines that employs the mild oxidant ^tBuOO^tBu along with the β -diketiminato Cu(I) catalyst [Cl₂NN]Cu (Scheme 2). A

Scheme 2. Catalytic C–H Amination with Alkyl and Arylamines



mechanistic study of the reaction revealed two key stoichiometric transformations: (a) generation of the copper(II) alkoxide [Cu^{II}]-O^tBu upon reaction of [Cu^I] with ^tBuOO^tBu and (b) acid–base chemistry with an amine to generate the copper(II) amide [Cu^{II}]-NHAd that participates in stoichiometric C–H amination of C–H substrates, such as indane and ethylbenzene.¹³

While organic peroxides such as ^tBuOO^tBu have been widely used for selective catalytic oxidation of hydrocarbons, few investigations focus on mechanistic aspects of peroxide activation. Such studies are critical to develop novel oxidation catalysts of more inert hydrocarbon substrates given that the homolytic BDE of ^tBuO–H rivals that of C–H bonds in methane (104 kcal/mol).⁶ Scarce mechanistic studies have focused on the activation of dialkyl peroxides at Cu(I),^{15,16} although they have been noted to react more sluggishly than

Received: June 3, 2012

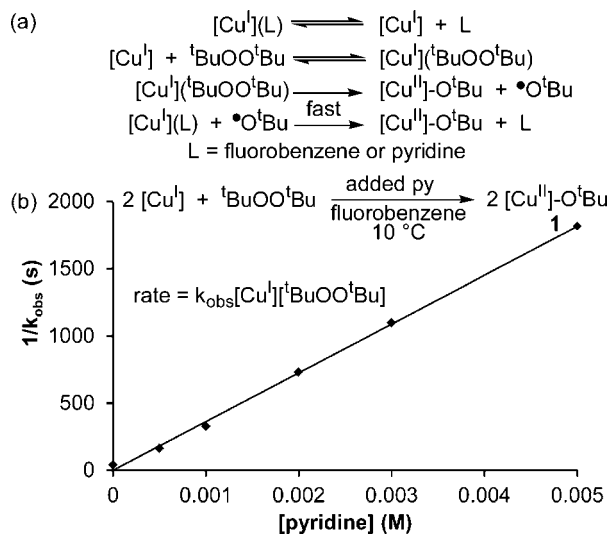
Published: September 25, 2012

their peroxyester counterparts^{15,17} for which no accurate kinetic data are known.¹⁸ The hydroperoxides HOO^tBu and HOOH react with aqueous Cu⁺ giving first-order behavior in both Cu⁺ and oxidant with rate constants $k \approx 4 \times 10^3 \text{ M}^{-1} \text{ s}^{-1}$ at 25 °C.¹⁹ To better understand the activation and roles of ^tBuOO^tBu in this and other Cu-based C–H functionalization systems,^{11,20} we undertook an integrated experimental–theoretical investigation involving the reaction between ^tBuOO^tBu and [Cu^I].

Addition of 20 equiv of ^tBuOO^tBu to [Cu^I] (initially 0.50 mM) in fluorobenzene over –20 to +20 °C results in rapid, quantitative conversion to [Cu^{II}–O^tBu] (**1**), which has a strong optical band at $\lambda_{\text{max}} = 481 \text{ nm}$ ($\epsilon = 3560 \text{ M}^{-1} \text{ cm}^{-1}$). To avoid photochemical dissociation of ^tBuOO^tBu (optically silent above $\lambda = 350 \text{ nm}$), we followed the reactions at a single wavelength ($\lambda = 481 \text{ nm}$) in an otherwise dark environment. In each case, first-order growth of **1** takes place affording the pseudo-first-order rate constant k_{obs} . The linear plot of k_{obs} vs [^tBuOO^tBu] at 10 °C (Figure S3) indicates a second-order overall rate law: $\text{rate} = k[\text{Cu}^{\text{I}}][^t\text{BuOO}^t\text{Bu}]$.

Second-order rate constants for the oxidation of [Cu^I] by ^tBuOO^tBu in fluorobenzene span 0.13(2) to 5.9(2) M^{–1} s^{–1} over the temperature range –20 to +20 °C (Table S2) corresponding to activation parameters $\Delta H^\ddagger = 13.6(4) \text{ kcal/mol}$ and $\Delta S^\ddagger = 8.3(1.4) \text{ e.u.}$ with $\Delta G^\ddagger(298 \text{ K}) = 16.1(5) \text{ kcal/mol}$. The near-zero entropy of activation in this bimolecular reaction supports a role for fluorobenzene dissociation from [Cu^I] preceding the activation of ^tBuOO^tBu that results in the formation of **1** and ^tBuO[•]. The *tert*-butoxy radical is presumably rapidly captured by [Cu^I] in solution to form another equivalent of [Cu^{II}–O^tBu] (Scheme 3a, L = fluorobenzene).

Scheme 3. (a) Mechanistic and (b) Kinetic Analysis of Oxidation of [Cu^I] by ^tBuOO^tBu in the Presence of Pyridine



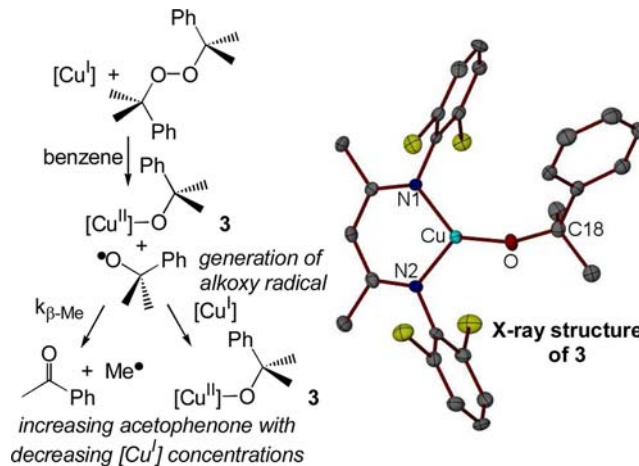
To probe the requirement for ligand dissociation from [Cu^I] prior to interaction with ^tBuOO^tBu (Scheme 3), kinetic studies were performed with varying amounts of pyridine, which binds reversibly to the [Cu^I] fragment. Addition of excess pyridine to {[Cu^I]₂(μ -benzene)} in ether allows for isolation and crystallization of [Cu^I](py) (**2**). The X-ray structure of **2** (Figure S29) is similar to those of related β -diketiminato Cu(I) pyridine adducts^{21,22} such as [Me₂NN]Cu(2,4-lutidine).²² Based on the shoulder at $\lambda = 416 \text{ nm}$ in the UV–vis spectrum of [Cu^I](py), which is absent in [Cu^I](η^2 -C₆H₅F) (Figures S7–

S9), we obtain thermodynamic parameters $\Delta H = -0.6(1) \text{ kcal/mol}$, $\Delta S = 1.3(1) \text{ e.u.}$ with $\Delta G_{298} = -0.9(1) \text{ kcal/mol}$ for binding of pyridine, which includes loss of fluorobenzene.

Addition of pyridine (1–10 equiv) at 10 °C slows the first-order growth of [Cu^{II}–O^tBu] in the reaction of [Cu^I] (initially 0.50 mM) and ^tBuOO^tBu (20 equiv) (Scheme 3, L = py). A plot of $1/k_{\text{obs}}$ vs [pyridine] gives a straight line (Scheme 3b) indicating an inverse first-order dependence on pyridine. The presence of 10 equiv of pyridine leads to a 47-fold reduction in rate as compared to comparable pyridine-free conditions. These observations signal the importance of pyridine dissociation from [Cu^I] during reaction with ^tBuOO^tBu (Scheme 3). We note that pyridine also binds to the copper(II) alkoxide [Cu^{II}–O^tBu], albeit weakly, shown by a shift in the optical band of **3** at 481 nm that moves to 496 nm with excess pyridine (40 equiv and more) accompanied by a reduction in intensity (Figure S14).

The reaction of [Cu^I] with dicumyl peroxide provides further evidence for the formation of alkoxy radicals RO[•] in the reaction between [Cu^I] and dialkyl peroxides ROOR. Facile unimolecular decomposition of the cumyloxy radical PhMe₂CO[•] to acetophenone and a methyl radical ($k = 3.7(5) \times 10^5 \text{ s}^{-1}$ in benzene at 30 °C; Scheme 4)²³ provides

Scheme 4. Generation and Competitive Capture of the [•]O₂CMe₂Ph Radical by [Cu^I]



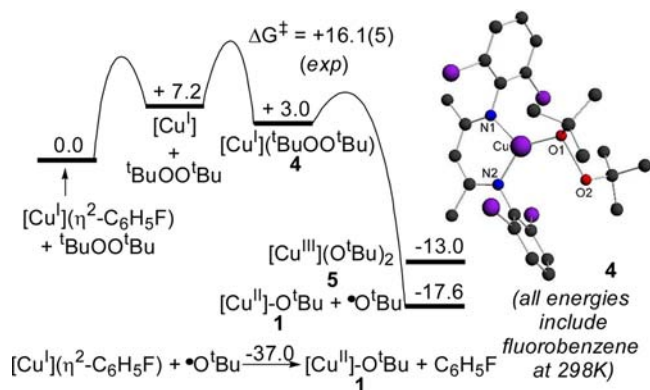
a convenient probe for the presence of alkoxy radicals. Reaction of {[Cl₂NN]Cu}₂(benzene) with 4 equiv of dicumyl peroxide in fluorobenzene at rt allows for the isolation of [Cu^I–O₂CMe₂Ph] (**3**) as red crystals of **3**· $\frac{1}{2}$ (dicumyl peroxide) from pentane. The structure of **3** shows a slightly distorted trigonal planar geometry with N1–Cu–O1 and N2–Cu–O1 angles of 134.50(9)° and 129.02(10)° along with a short Cu–O bond length of 1.788(2) Å. These values are very similar to those found in the structure of previously reported **1** (134.04(9)°, 129.64(9)°, and 1.785(2) Å, respectively).¹³ In fluorobenzene, **3** exhibits closely related optical absorption ($\lambda_{\text{max}} = 467 \text{ nm}$, $\epsilon = 3760 \text{ M}^{-1} \text{ cm}^{-1}$) and EPR spectra (Figures S15–S16 and S27–S28, respectively).

The reaction between [Cu^I] (initially 0.50 mM) and 20 equiv of dicumyl peroxide in fluorobenzene at 10 °C gives **3** under pseudo-first-order kinetics with an overall second-order rate constant $k = 0.79(5) \text{ M}^{-1} \text{ s}^{-1}$. This is about three times slower compared to the analogous reaction with ^tBuOO^tBu, reflecting the added steric bulk of dicumyl peroxide vs di-*tert*-

butylperoxide. Reaction of $[\text{Cu}^{\text{I}}]$ and dicumyl peroxide in a 1:2 molar ratio at rt in benzene- d_6 reveals that acetophenone forms, suggesting the intermediacy of the $\text{PhMe}_2\text{CO}^\bullet$ radical (Scheme 4). Notably, the amount of acetophenone formed decreases with increasing initial $[\text{Cu}^{\text{I}}]$ concentration, indicating more efficient trapping of the $\text{PhMe}_2\text{CO}^\bullet$ radical at higher $[\text{Cu}^{\text{I}}]$ concentrations. For instance, with an initial $[\text{Cu}^{\text{I}}]$ concentration of 0.01 M, acetophenone is produced in 71(2)% yield whereas an initial $[\text{Cu}^{\text{I}}]$ concentration of 0.04 M gives a 26(2)% yield of acetophenone. Based on these data and the rate of β -Me scission for $\text{PhMe}_2\text{CO}^\bullet$,²³ we can crudely estimate the rate of bimolecular trapping of the cumyloxy radical by $[\text{Cu}^{\text{I}}]$ in benzene at rt to be on the order of $2 \times 10^7 \text{ M}^{-1} \text{ s}^{-1}$.

We employed theory to provide deeper insight into the reaction between $[\text{Cu}^{\text{I}}]$ and ${}^t\text{BuOO}{}^t\text{Bu}$. Binding of fluorobenzene (η^2 -CC) and pyridine (κ^1 -N) to the naked, two-coordinate $[\text{Cu}^{\text{I}}]$ fragment is exergonic by 7.2 and 16.7 kcal/mol, respectively. DFT calculations of the putative intermediate $[\text{Cu}^{\text{I}}]({}^t\text{BuOO}{}^t\text{Bu})$ (**4**) reveal a minimum that is 3.0 kcal/mol higher in free energy than the $[\text{Cu}^{\text{I}}](\eta^2\text{-C}_6\text{H}_5\text{F})$ species. Loss of ${}^t\text{BuO}^\bullet$ from adduct **4** to give $[\text{Cu}^{\text{II}}]\text{-O}{}^t\text{Bu}$ (**1**) + ${}^t\text{BuO}^\bullet$ is calculated to result in a ΔG_{rxn} (298 K) of -20.6 kcal/mol (Scheme 5).

Scheme 5. DFT Energies and Structure of **4**

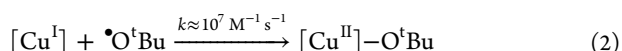
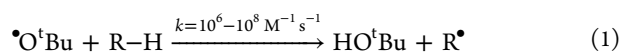


A diamagnetic square planar copper(III) bis(*tert*-butoxide) complex $[\text{Cu}^{\text{III}}](\text{O}{}^t\text{Bu})_2$ (**5**) representing the formal oxidative addition of ${}^t\text{BuOO}{}^t\text{Bu}$ to $[\text{Cu}^{\text{I}}]$ was also found via simulation. Although **5** is considerably lower in free energy than the adduct **4** by 17 kcal/mol, species **5** nonetheless is predicted to be unstable by 4.6 kcal/mol in free energy toward loss of the ${}^t\text{BuO}^\bullet$ radical to give **1**. The endothermic ($\Delta H = +15.0$ kcal/mol) fragmentation $\mathbf{5} \rightarrow \mathbf{1} + {}^t\text{BuO}^\bullet$ is strongly entropically driven ($-T\Delta S = -19.6$ kcal/mol at 298 K). Addition of ${}^t\text{BuO}^\bullet$ to $[\text{Cu}^{\text{I}}](\eta^2\text{-C}_6\text{H}_5\text{F})$ to give **1** + fluorobenzene is extremely exergonic with a calculated ΔG_{rxn} of -37.0 kcal/mol. Thus, the ${}^t\text{BuO}^\bullet$ radical formed in the reaction of $[\text{Cu}^{\text{I}}]$ with ${}^t\text{BuOO}{}^t\text{Bu}$ is likely to be rapidly captured by another equivalent of $[\text{Cu}^{\text{I}}]$.

Based on experimental and theoretical considerations, we propose that the rate-determining step in the reaction of ${}^t\text{BuOO}{}^t\text{Bu}$ with $[\text{Cu}^{\text{I}}]$ is the generation of the peroxide adduct $[\text{Cu}^{\text{I}}]({}^t\text{BuOO}{}^t\text{Bu})$ (**4**, Schemes 3 and 5) from a $[\text{Cu}^{\text{I}}](\text{L})$ species ($\text{L} = \eta^2$ -fluorobenzene or pyridine). This peroxide adduct **4** is primed for loss of the ${}^t\text{BuO}^\bullet$ radical. While we have been unable to find a transition state for the loss of ${}^t\text{BuO}^\bullet$ from **4**, potential energy scans indicate that further lengthening of the O–O bond in **4** and a Cu–O bond in **5** result in flat

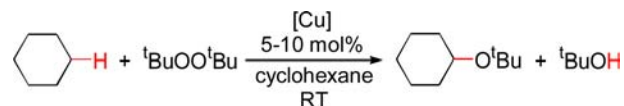
potential energy surfaces for the conversion of **4** to **5** (or $\mathbf{1} + {}^t\text{BuO}^\bullet$) and the dissociation of ${}^t\text{BuO}^\bullet$ from **5**, respectively (Figures S34–S35). The large drop in free energy associated with the loss of ${}^t\text{BuO}^\bullet$ from **4** and the correlation between lower reaction rates in the presence of py strongly suggest that the rate-determining step in the formation of **1** from the $[\text{Cu}^{\text{I}}](\text{L})$ species and ${}^t\text{BuOO}{}^t\text{Bu}$ corresponds to competition between ${}^t\text{BuOO}{}^t\text{Bu}$ and L for coordination to the $[\text{Cu}^{\text{I}}]$ fragment (Scheme 3a).

These results point to the kinetically facile and thermodynamically favorable generation of alkoxy radicals by the $[\text{Cu}^{\text{I}}]({}^t\text{BuOO}{}^t\text{Bu})$ system, suggesting that ${}^t\text{BuO}^\bullet$ may participate in HAA in C–H functionalization catalysis. Second-order rate constants for HAA reactions of benzylic and unactivated sp^3 C–H substrates R–H by ${}^t\text{BuO}^\bullet$ at rt span ca. $10^{6-8} \text{ M}^{-1} \text{ s}^{-1}$ (eq 1), comparable to our estimate for trapping of $\text{PhMe}_2\text{CO}^\bullet$ by $[\text{Cu}^{\text{I}}]$ (eq 2). Low concentrations of $[\text{Cu}^{\text{I}}]$ present in catalytic C–H functionalization reactions (~ 1 mM),^{13,14} however, may bias the ${}^t\text{BuO}^\bullet$ radical toward productive HAA with R–H to give R^\bullet vs capture by $[\text{Cu}^{\text{I}}]$ to give **1**.



To illustrate the potential for the ${}^t\text{BuO}^\bullet$ radical generated upon reaction of $[\text{Cu}^{\text{I}}]$ with ${}^t\text{BuOO}{}^t\text{Bu}$ to engage in HAA of a substrate R–H, we employed cyclohexane as a solvent and substrate which undergoes facile HAA by ${}^t\text{BuO}^\bullet$ ($k = 8.1 \times 10^5 \text{ M}^{-1} \text{ s}^{-1}$ in a 2:1 ${}^t\text{BuOO}{}^t\text{Bu}$ /benzene mixture at 25 °C).⁵ Reaction of $[\text{Cu}^{\text{I}}]$ (6.7 mM) with ${}^t\text{BuOO}{}^t\text{Bu}$ (10 equiv) in cyclohexane at rt for 24 h gave a 50% yield of the ether Cy–O ${}^t\text{Bu}$ (Scheme 6). Extending the reaction time to 72 h

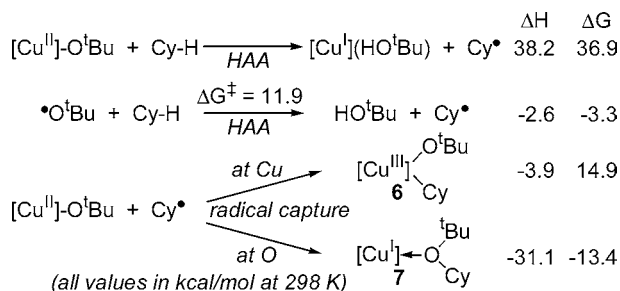
Scheme 6. Catalytic C–H Etherification with ${}^t\text{BuOO}{}^t\text{Bu}$



increased the yield to 60% employing only 5 mol % $[\text{Cu}^{\text{I}}]$ (3.3 mM) (Table S6). The observation of the C–H functionalized product suggests that the ${}^t\text{BuO}^\bullet$ radical generated upon reaction of ${}^t\text{BuOO}{}^t\text{Bu}$ with $[\text{Cu}^{\text{I}}]$ abstracts a H-atom from the strong C–H bond of cyclohexane (C–H BDE ≈ 97 kcal/mol) to give the cyclohexyl radical Cy^\bullet . Control experiments reveal that the copper(II) alkoxide **1** does not engage in HAA with cyclohexane (Cy–H) under these conditions. After 17 h at rt in cyclohexane, very little decay (3.5%) of **1** occurs. Akin to the Kharasch–Sosnovsky reaction with peroxyesters (Scheme 1), we hypothesize that C–O bond formation results from capture of the Cy^\bullet radical by the $[\text{Cu}^{\text{II}}]\text{-O}{}^t\text{Bu}$ intermediate (Scheme 7). Since the ${}^t\text{BuO}^\bullet$ radical undergoes unimolecular β -scission with $k = 2.0(4) \times 10^4 \text{ s}^{-1}$ in benzene at 25 °C,²⁴ it is unlikely that a significant amount of Cy–O ${}^t\text{Bu}$ results from the direct coupling of highly reactive Cy^\bullet and ${}^t\text{BuO}^\bullet$ radicals present in minute concentrations in solution.

We employed theory to examine this reaction in detail. Consistent with experiment, HAA of Cy–H by $[\text{Cu}^{\text{II}}]\text{-O}{}^t\text{Bu}$ is very disfavored ($\Delta G(298 \text{ K}) = 36.9$ kcal/mol) and not expected to occur under mild conditions. In contrast, HAA of Cy–H by ${}^t\text{BuO}^\bullet$ is calculated to proceed with a low activation barrier $\Delta G^\ddagger(298 \text{ K}) = 11.9$ kcal/mol (exp = $9.4(7)$ kcal/mol)⁵

Scheme 7. C–H Etherification: Theory



and is thermodynamically favored due to the high ${}^t\text{BuO-H}$ bond strength. We then considered the thermodynamics of two possible pathways for the formation of the $\text{Cy-O}^t\text{Bu}$ bond via capture of Cy^\bullet by $[\text{Cu}^{\text{II}}]\text{-O}^t\text{Bu}$. Direct addition to the Cu center to give the square planar copper(III) organometallic $[\text{Cu}^{\text{III}}](\text{Cy})(\text{O}^t\text{Bu})$ (6) is enthalpically favorable ($\Delta H = -3.9$ kcal/mol), but entropically unfavorable ($\Delta S = 63.1$ e.u.) leading to an overall endergonic transformation ($\Delta G(298\text{ K}) = +14.9$ kcal/mol). On the other hand, direct capture of Cy^\bullet at the O-atom of 3 to form the copper(I) ether adduct $[\text{Cu}^{\text{I}}](\text{O}(\text{Cy})^t\text{Bu})$ (7) is thermodynamically favorable with $\Delta G(298\text{ K}) = -13.4$ kcal/mol. As a result, C–O reductive elimination from putative 6 to form the product ether $\text{Cy-O}^t\text{Bu}$ bound to $[\text{Cu}^{\text{I}}]$ is highly favored ($\Delta G(298\text{ K}) = -28.3$ kcal/mol).

The ability of low concentrations of $[\text{Cu}^{\text{I}}]$ (e.g., 1 mM) to generate the highly potent radical ${}^t\text{BuO}^\bullet$ at rates ca. 10^9 faster than the uncatalyzed thermal homolytic cleavage of ${}^t\text{BuOO}^t\text{Bu}$ at τ^{25} opens the possibility of efficient HAA reactions with substrates R–H containing unactivated sp^3 -hybridized C–H bonds under mild conditions. Importantly, the $[\text{Cu}^{\text{II}}]\text{-O}^t\text{Bu}$ species formed alongside the ${}^t\text{BuO}^\bullet$ radical is capable of capturing the C-centered radical Cy^\bullet to form a new C–O bond in $\text{Cy-O}^t\text{Bu}$. In contrast to the common use of peroxesters $\text{RC}(\text{O})\text{OO}^t\text{Bu}$ with allylic substrates to give the corresponding allylic carboxylates (Scheme 1), catalytic ether formation at sp^3 C–H bonds with organoperoxides is rare.²⁶ Moreover, facile acid–base chemistry available to the $[\text{Cu}^{\text{II}}]\text{-O}^t\text{Bu}$ intermediate 1 with substrates H–FG such as amines H–NR¹R² to form copper amides $[\text{Cu}]\text{-NR}^1\text{R}^2$ (Scheme 2) may allow for the development of a family of sp^3 C–H functionalization protocols that deliver products R–FG in new variations of the Kharasch–Sosnovsky reaction.

■ ASSOCIATED CONTENT

Supporting Information

Experimental, characterization, and calculational details (PDF) and X-ray crystallographic data (CIF). This material is available free of charge via the Internet at <http://pubs.acs.org>.

■ AUTHOR INFORMATION

Corresponding Author

thw@georgetown.edu; t@unt.edu

Notes

The authors declare no competing financial interest.

■ ACKNOWLEDGMENTS

T.H.W. is grateful to the NSF (CHE-1012523) and Georgetown thanks the NSF (CHE-0840453) for the award of an EPR spectrometer. T.R.C. and C.L.M. thank the NSF for support via

Grant CHE-1057785. We thank Dr. Matthew S. Varonka for assistance in the collection of the X-ray of 2 and Martina Käbß for acquiring the low temp EPR spectra of 1 + py.

■ REFERENCES

- (1) (a) Yeung, C. S.; Dong, V. M. *Chem. Rev.* **2011**, *111*, 1215–1292. (b) Lie, C.; Zhang, H.; Lei, A. *Chem. Rev.* **2011**, *111*, 1780–1824. (c) Li, C.-J. *Acc. Chem. Res.* **2009**, *2009*, 335–344.
- (2) (a) Kharasch, M. S.; Sosnovsky, G. *J. Am. Chem. Soc.* **1958**, *80*, 756. (b) S., M.; Sosnovsky, G. *J. Am. Chem. Soc.* **1959**, *81*, 5819–5824. (3) (a) Andrus, M. B.; Lashley, J. C. *Tetrahedron* **2002**, *58*, 845–866. (b) Rawlins, D. J.; Sosnovsky, G. *Synthesis* **1972**, 1–28. (c) Beckwith, A. L. J.; Zavitsas, A. A. *J. Am. Chem. Soc.* **1986**, *108*, 8230–8234.
- (4) Eames, J.; Watkinson, M. *Angew. Chem., Int. Ed.* **2001**, *40*, 3567–3571.
- (5) Finn, M.; Friedline, R.; Suleman, N. K.; Wohl, C. J.; Tanko, J. M. *J. Am. Chem. Soc.* **2004**, *126*, 7578–7584.
- (6) Luo, Y.-R. *Handbook of Bond Dissociation Energies in Organic Compounds*; CRC Press: Boca Raton, FL, 2002.
- (7) (a) Andrus, M. B.; Zhou, Z. *J. Am. Chem. Soc.* **2002**, *124*, 8806–8807. (b) Sekar, G.; DattaGupta, A.; Singh, V. K. *J. Org. Chem.* **1998**, *62*, 2961–2967.
- (8) Hoang, V. D. M.; Reddy, P. A. N.; Kim, T.-J. *Organometallics* **2008**, *27*, 1026–1027.
- (9) Speier, G.; Fülöp, V. *J. Chem. Soc., Chem. Commun.* **1990**, 905–906.
- (10) Santoro, S.; Liao, R.-Z.; Himo, F. *J. Org. Chem.* **2011**, *76*, 9246–9252.
- (11) Shuai, Q.; Deng, G.; Chua, Z.; Bohle, D. S.; Li, C.-J. *Adv. Synth. Catal.* **2010**, *352*, 632–636.
- (12) Mayoral, J. M.; Rodríguez-Rodríguez, S.; Salvatella, L. *Chem.—Eur. J.* **2008**, *14*, 9274–9285.
- (13) Wiese, S.; Badié, Y. M.; Gephart, R. T.; Mossin, S.; Varonka, M. S.; Melzer, M. M.; Meyer, K.; Cundari, T. R.; Warren, T. H. *Angew. Chem., Int. Ed.* **2010**, *49*, 8850–8855.
- (14) Gephart, R. T.; Huang, D. L.; Aguila, M. J. B.; Schmidt, G.; Shahu, A.; Warren, T. H. *Angew. Chem., Int. Ed.* **2012**, *51*, 6488–6492.
- (15) Kochi, J. K. *J. Am. Chem. Soc.* **1963**, *85*, 1958–1968.
- (16) Morris, G. E.; Oakley, D.; Pippard, D. A.; Smith, D. J. H. *J. Chem. Soc., Chem. Commun.* **1987**, 410–411.
- (17) Bemis, A.; Kochi, J. K. *Tetrahedron* **1968**, *24*, 5099–5113. Speier, G. *Inorg. Chim. Acta* **1988**, *143*, 149–150.
- (18) Smith, K.; Hupp, C. D.; Allen, K. L.; Slough, G. A. *Organometallics* **2005**, *24*, 1747–1755.
- (19) Masarwa, M.; Cohen, H.; Meyerstein, D.; Hickman, D. L.; Bakac, A.; Espenson, J. H. *J. Am. Chem. Soc.* **1988**, *110*, 4293–4297.
- (20) (a) Chu, L.; Qing, F.-L. *J. Am. Chem. Soc.* **2012**, *134*, 1298–1304. (b) Bi, H.-P.; Zhao, L.; Liang, Y.-M.; Li, C.-J. *Angew. Chem., Int. Ed.* **2009**, *48*, 792–795.
- (21) Lee, W.-Z.; Tolman, W. B. *Inorg. Chem.* **2002**, *41*, 5656–5658.
- (22) Amisial, L. D.; Dai, X.; Kinney, R. A.; Krishnaswamy, A.; Warren, T. H. *Inorg. Chem.* **2004**, *43*, 6537–6539.
- (23) Avila, D. V.; Brown, C. E.; Ingold, K. U.; Luszyk, J. *J. Am. Chem. Soc.* **1993**, *115*, 466–470.
- (24) Weber, M.; Fischer, H. *J. Am. Chem. Soc.* **1999**, *1999*, 7381–7388.
- (25) *Polymer Handbook*; Brandrup, J.; Immergut, E. H.; Grulke, E. A., Eds.; John Wiley: New York, 1999, II/23–26.
- (26) (a) Story, P. R. *J. Org. Chem.* **1961**, *26*, 287–290. (b) Brennan, M. E.; Battiste, M. A. *J. Org. Chem.* **1968**, *33*, 324–332.